Computer simulation of diffusion-limited cluster-cluster aggregation with an Epstein drag force

F. Pierce, C. M. Sorensen, and A. Chakrabarti
Department of Physics, Kansas State University, Manhattan, Kansas 66506, USA
(Received 25 April 2006; revised manuscript received 18 July 2006; published 25 August 2006)

The motion of particles, dispersed in a medium, between collisions with each other can, in limiting situations, be either ballistic (straight line) or diffusive (random walker). The diffusive regime can be divided into two distinct subregimes. The "continuum regime" exhibits Stokes-Einstein-type diffusion (no-slip surface boundary condition) with a frictional coefficient proportional to the particle size (linear dimension). The "Epstein regime," as we shall refer to it, is characterized by a frictional coefficient proportional to the particle cross-sectional area, hence an Epstein-type diffusion (slip surface). The purpose of the current study is to illuminate the dynamics of *dilute-limit* aggregation in the Epstein regime. We present results from low volume fraction Monte Carlo simulations of cluster-cluster aggregation in the Epstein regime with the particle motion based on each particle's cross-sectional area. Our findings indicate that aggregates grown under Epstein conditions have a fractal dimension of ~ 1.8, similar to that of diffusion-limited cluster-cluster aggregates (DLCA) in the continuum regime. The kinetic exponent z in the Epstein regime is found to be $z \approx 0.8$, lower than its value for both the continuum regime DLCA ($z=1$) and for the ballistic cluster aggregation regime ($z \approx 2$). Cluster size distribution data for Epstein systems are found to scale at large cluster sizes with exponents consistent with the kinetic data. A scaling argument for predicting the kinetic exponent and kernel homogeneity based on the mass or size dependence of the particle velocity and collision cross section is presented and is seen to give accurate results for dilute and intermediate values of particle volume fractions not only for the current study, but also for work done by other researchers with various choices for the aggregation kernel.

DOI: 10.1103/PhysRevE.74.021411 PACS number(s): 61.43.Hv, 66.10.Cb, 51.20.+d

I. INTRODUCTION

The utility of aggregation to our current technology cannot be overstated, including applications in biological gels, pharmaceuticals, chemical production, aerogel and xerogel light weight materials, and numerous foods [1,2]. Aggregation in colloids and aerosols has been extensively studied both theoretically and under a host of experimental conditions (premixed flames, diffusion-limited and reaction-limited colloidal suspensions, etc.) [3–16].

Aggregation kinetics is governed by the Smoluchowski equation, which describes the rate of change of the concentration, $n_k(t)$, of particles containing k monomers as

$$\frac{dn_k}{dt} = \sum_{i=1}^{k-1} K(i,k-i) n_i n_{k-i} - n_k \sum_{i=1}^{\infty} K(i,k) n_i. \tag{1}$$

The aggregation kernel $K(i,j)$ expresses the rate of aggregation between particles of size (number of monomers) i with particles of size j. The Smoluchowski equation is a mean-field equation because it assumes that the probability of two particles meeting is simply proportional to the product of their number densities, i.e., there are no spatial correlations between particles.

In many physical situations, K is a time-independent homogeneous function of particle size, i.e.,

$$K(ai,aj) = a^{\lambda} K(i,j), \tag{2}$$

where λ is the degree of homogeneity. Then the Smoluchowski equation yields self-preserving, scaling solutions for n_k. A self-preserving distribution does not change in shape; all the time dependence is in the mean cluster size. K is a power of the average particle size N for homogeneous kernels,

$$K \sim N^{\lambda} \tag{3}$$

The kinetic exponent z, which characterizes the power-law growth with time of the average particle mass, is related to the homogeneity λ by [5]

$$z = (1-\lambda)^{-1}. \tag{4}$$

It is well known that irreversible aggregation of solid particles leads to the formation of fractal aggregates [1,2,6] with a power-law relationship between the cluster radius of gyration R_g and the number of monomers N in a cluster,

$$N = k_0 \left(\frac{R_g}{a} \right)^{D_f}. \tag{5}$$

Here a is the radius of the primary particles, k_0 is a proportionality constant of the order unity, and D_f is the fractal dimension of the cluster. For diffusion-limited cluster-cluster aggregation (DLCA) in the continuum regime, $D_f \approx 1.8$ in three dimensions, while for ballistic cluster aggregation (BLCA), $D_f \approx 1.9$ [5,7]. Previous work from this lab has found $k_0 = 1.3 \pm 0.1$ for DLCA aggregates in three dimensions [17,18] from both simulations and transmission electron microscopy (TEM) measurements of soot aggregates.

The purpose of this paper is to elucidate the process of aggregation in what we call the "Epstein regime," a diffusional regime where the diffusion coefficient is inversely proportional to the cluster projected area. Aerosols can aggregate via DLCA, with either Stokes-Einstein or Epstein diffusion, BLCA, or in regions that crossover between these major regimes. Colloids are, for all practical purposes, en-

tirely in the regime of Stokes-Einstein diffusion where $D \sim R^{-1}$ to yield either continuum DLCA, if the cluster slicking probability is 1, or reaction-limited cluster-cluster aggregation (RLCA), if the sticking probability is significantly less than 1.

Our recent work [19–23] has shown that the particle volume fraction affects the aggregation when the system becomes crowded. To describe "crowded" we have used the mean particle-particle nearest-neighbor distance R_{nn}, which is related to the volume fraction. We then define a *cluster dilute regime* as one in which the relative separation to size ratio is large, i.e., $R_{\mathrm{nn}}/R_g \gg 1$, and a *cluster dense regime* for which the separation is relatively small, i.e., $R_{\mathrm{nn}}/R_g \geqslant 1$. In this work, we also need to define an intermediate regime between cluster dilute and cluster dense.

We will present scaling arguments for the homogeneity of the aggregation kernel for all regimes. This leads directly to exponents describing the kinetics, and the size distribution. After these general studies, we will present simulations of aggregation in the Epstein regime. Simulations yield particle morphology, kinetics, and size distributions. We find that the particle morphology is the same as found for Stokes-Einstein diffusion ("normal" DLCA). We then determine the relationship between projected area and number of monomers per aggregate, N. This is relevant to the drag the aggregate particle experiences in the medium. Finally, we determine that the kinetics and size distribution exponents are different from either normal DLCA or BLCA, but agree with our scaling analysis.

II. AGGREGATION REGIMES

The aggregation kernel is sensitive to the motion of the particles between interparticle collisions, whether diffusive or ballistic. The aggregation rate, size distribution, and particle morphology are all functions of this motion.

To describe particle motion in a medium, hence the aggregation regime, the most commonly used parameter is the Knudsen number $\mathrm{Kn}=\lambda_m/R$, the ratio of the mean free path of the medium molecules λ_m to the particle radius R. To a good approximation $\lambda_m \sim n_m^{-1}$, with n_m the medium molecule number density, which for a gas is temperature- and pressure-dependent [1].

Often overlooked is the diffusional Knudsen number $\mathrm{Kn}_D=\lambda_p/R$, where λ_p is the persistence length of the particle. λ_p is the distance over which a particle moves *effectively* in a straight line [24]. If one observes a particle's motion on scales much less than λ_p, the motion is essentially ballistic, while for larger length scales the path is diffusional (random walker).

Friedlander, Hidy, and others refer to the $\mathrm{Kn} \ll 1$ range as the "continuum regime" [1,25]. Fuchs refers to this as the "Stokes" or "hydrodynamic regime" of motion, where particle motion disturbs the "isotropism of the distribution of molecular velocities within the medium" [26]. Many authors, including those above, do not directly refer to a specific condition on Kn_D. As noted by Oh and Sorensen, both $\mathrm{Kn} \sim 0$ and $\mathrm{Kn}_D \sim 0$ in the continuum [15]. Many aggregation studies are carried out in this continuum regime where the particle motion is diffusive between collisions. These include colloidal aggregation in a liquid medium and aerosol aggregation at relatively low temperatures (or high pressures) and/or large particle sizes. The continuum regime diffusion constant for *spherical* particles is given by the Stokes-Einstein relation

$$D_{\mathrm{SE}} = \frac{k_B T}{6\pi\eta R}, \tag{6}$$

where k_B is Boltzmann's constant, T is the temperature, and η is the viscosity of the medium. Thus $D \sim R^{-1}$ in the continuum limit.

The other extreme ($\mathrm{Kn} \gg 1$) is the free molecular regime. Friedlander describes it as the regime where the particle has little effect on the medium since most of the molecules impacting the particle surface come from far away in the medium and rarely collide with those just leaving the surface [1]. Fuchs has a similar description [26]. In this regime, a *spherical* particle experiences a drag force whose coefficient is given by Epstein's Eq. (1),

$$f = \frac{8}{3} R^2 \rho \left(\frac{2\pi k_B T}{m}\right)^{1/2} \left(1 + \frac{\beta\pi}{8}\right) \tag{7}$$

where ρ is the medium mass, m is the gas molecular mass, and β is the momentum accommodation coefficient ($0 < \beta < 1$). β refers to the fraction of molecules that "diffusively" leave the surface of the particle after collision uncorrelated with their incoming trajectory. Typically $\beta = 0.91$, but the exact value of β is not relevant for our study [15,1]. The R^2 dependence is a result of the cross-sectional area of the sphere in the gas medium [26].

Free-molecular particles can move either diffusively or ballistically between collisions. Previous workers have claimed that a crossover between these two extremes occurs when $\mathrm{Kn}_D \approx 1$ [15,24,26]. We feel, however, that a better determination of this crossover would be to compare the particle persistence length to the nearest-neighbor separation, and hence define a nearest-neighbor Knudsen number as $\mathrm{Kn}_n = \lambda_p/R_{\mathrm{nn}}$.

When $\mathrm{Kn}_n < 1$, the motion of spherical particles in the free molecular regime is diffusive, and the diffusion constant is found through Eq. (7) as

$$D_{E_P} = \frac{3}{8\rho R^2} \left(\frac{m k_B T}{2\pi}\right)^{1/2} \left(1 + \frac{\pi}{8}\beta\right)^{-1}. \tag{8}$$

Thus diffusion in the Epstein regime is characterized by $D \sim R^{-2}$.

As Kn increases from ~0 to higher values, the crossover from the continuum to Epstein diffusion occurs. This intermediate Kn regime is usually called the "slip regime," which can be described through the use of the Cunningham correction, $C(\mathrm{Kn})$, to the Stokes-Einstein diffusion law

$$D = D_{\mathrm{SE}} C(\mathrm{Kn}), \tag{9a}$$

$$C(\mathrm{Kn}) = 1 + 1.257\mathrm{Kn} + 0.4\exp(-1.1/\mathrm{Kn}) \tag{9b}$$

or simply and equivalently

$$D = D_{SE} + D_{E_p}. \tag{9c}$$

Equation (9c) is a simple alternative to Eqs. (9a) and (9b) that agrees with them to 4% or better [27]. The $Kn \to 0$ limit of D is then D_{SE}. Fuchs' formula for the viscosity of a gas gives $\eta = 0.3502 n_m m v \lambda_m$, where n_m is the medium gas number density and v is the thermal velocity of the gas molecules [26]. Using this formula, the $Kn \gg 1$ limit yields $D = D_{E_p}$ with D_{E_p} given by Eq. (8) with $\beta = 0.91$. Values of the diffusion constant derived from Eqs. (9a)–(9c) are at least 10% different from these limits when $0.1 \leqslant Kn \leqslant 10$, which conveniently defines the slip regime.

We will use the term "ballistic regime" when the motion of the particle between interparticle collisions is a straight line (i.e., when $Kn_n \gg 1$) and particles move with an rms (root mean square) velocity v of a particle of mass m given by

$$v = \left(\frac{3k_B T}{m}\right)^{1/2}. \tag{10}$$

Interstellar dust as well as aerosol particles in low-pressure and/or high-temperature flames lie in the ballistic regime.

The differences between the Epstein regime and the ballistic regime are just as important as their similarities. In both cases, the resistance to the medium is of the form given by Eq. (7), with drag force proportional to particle cross-sectional area. In the Epstein regime, however, the sum of molecular impacts with the particle *is* sufficient to appreciably alter the direction of particle motion between interparticle collisions, thus leading to diffusional motion. A particle in the ballistic regime still encounters drag, but the molecular impacts are insufficient to significantly alter the particle's velocity, hence effective straight-line motion between collisions results.

Our focus in this paper is to elucidate the dilute limit behavior of aggregates in the Epstein regime. We study the aggregation kinetics, cluster size distributions, and aggregate morphology by carrying out off-lattice Monte Carlo simulations of irreversible cluster-cluster aggregation at low monomer volume fractions.

III. DIFFUSIVE MOBILITY OF FRACTAL AGGREGATES

To apply Eqs. (6) and (8), which are for spherical particles, to fractal aggregates, we replace the sphere radius R with an effective mobility radius R_m for the aggregate. R_m will be a function of monomer size and number of monomers per aggregate as

$$R_m \sim a N^x, \tag{11}$$

which defines x.

Wang and Sorensen [28] made a comprehensive study of diffusive mobility for all Kn that both reviewed earlier work and presented new data for fractal aggregates. They concluded that when $Kn \ll 1$ and $N \geqslant 110$, $R_m \sim R_g \sim N^{1/D_f}$. Hence, for $D_f = 1.8$, $x = 0.55$. However, when $N \leqslant 110$ a crossover to the $N = 1$ limit begins and then Wang and Sorensen concluded $x = 0.44 \pm 0.03$.

For the Epstein regime, $Kn > 10$ and the drag force F_{drag} on a particle is proportional to its cross-sectional area A_{CS} as seen by the medium. From this a mobility radius R_m can be defined as

$$A_{CS} = \pi R_m^2. \tag{12}$$

Most particles have some degree of "drag screening." That is, part of the particle shields other parts from direct contact with fluid flow and thus the influence of gas drag.

Wang and Sorensen [28] considered both mobility measurements for fractals and various studies of monomer-monomer screening within a cluster and consistently found a value of

$$x = 0.44 \pm 0.03. \tag{13}$$

By coincidence, this is the same value as found in the continuous limit for $N \leqslant 110$.

IV. SCALING ANALYSIS OF THE AGGREGATION KERNEL

In this section, we present a simple scaling analysis that describes the functionality of the aggregation kernel on its variables. This functionality is quantified by the kernel homogeneity, which in turn determines the size distribution and kinetics functionalities on their variables. We will do this for all motional regimes and in two concentration regimes: dilute and intermediate.

Our scaling argument for the collision kernel starts with the general statement that the rate at which two particles collide, K, is proportional to their relative collision cross-sectional area A and relative velocity, v, yielding

$$K \sim Av, \tag{14}$$

consistent with the units of $[L^3 t]$. Here A is distinct from the cross-sectional area A_{CS} as seen by the medium molecules in mobility radius calculations [Eq. (12)]; it refers instead to the effective area seen by another fractal particle during a collision process. One typically writes this as $A \sim R_g^2$, where R_g is the radius of gyration of a fractal cluster [29].

A. Ballistic regime

In the ballistic regime, $v \sim N^{-1/2}$ via the equipartition of energy, Eq. (10). Since $R_g \sim N^{1/D_f}$, one finds from Eq. (14) that $K \sim N^{2/D_f - (1/2)}$, hence

$$\lambda = \frac{2}{D_f} - \frac{1}{2} \text{ (ballistic)}. \tag{15}$$

If one uses the accepted value of $D_f = 1.9$ in the ballistic limit, one obtains $\lambda = 0.55$. This is translated into $z = 2.2$ [see Eq. (4)] in this limit. This value of z is consistent with simulation results [30].

B. Diffusion regime

In the diffusive cases, whether in continuum or in Epstein regimes, v becomes a *characteristic velocity relevant for diffusion*,

$$v \sim \frac{D}{R_c}, \tag{16}$$

where D is the diffusion constant and R_c is a characteristic diffusional length scale.

In the dilute limit, $\mathrm{Kn} \ll 1$, R_g is the only length scale in the system. Thus by Eq. (16), $v \sim D/R_g$. The persistence length in the continuum is microscopic and R_{nn} is very large, hence neither represents a valid length scale for this scaling. In addition, $A \sim R_g^2$ and $R_g \sim N^{1/D_f}$. Thus Eq. (14) yields $K \sim DR_g$, a result originally derived by Smoluchowski in a more rigorous fashion. In this case $D \sim 1/R_m$ and $R_m \sim R_g$ in the continuum limit. As a result, $D \sim 1/R_g$, which with $K \sim DR_g$ implies that K is a constant (independent of the particle mass or linear size), in turn leading to $\lambda = 0$ and $z = 1$ in the dilute limit of the continuum regime.

We can use a similar argument for computing λ and z in the Epstein regime. $K \sim DR_g$ is still satisfied as in the continuum case, but now $D \sim 1/R_m^2$ holds. Since $R_m \sim N^x$ and $R_g \sim N^{1/D_f}$, one finds

$$\lambda = \frac{1}{D_f} - 2x \text{ (dilute regime;Epstein)} \tag{17}$$

in the Epstein regime.

In many simulations of cluster-cluster aggregation, the system is not in the asymptotically dilute range (defined by $R_{nn} \to \infty$) as monomer volume fraction is typically $f_v \sim 0.01$ and rarely goes lower than $f_v = 0.001$. In the cases of high initial volume fractions, the system is already monomer-dense, and the dilute-limit predictions need to be adjusted accordingly. Even at low initial volume fractions, one should be aware that the system will become cluster-dense (R_{nn} on the order of R_g) or crowded as the system aggregates. In order to determine the crowding of the system, we find the occupied volume of the particles by first determining the radius of the sphere that effectively encloses each cluster, the so-called "perimeter radius," R_p. R_p is related to R_g in the following way: $R_p = (1 + 2/D_f)^{1/2} R_g$ [15]. Since the volume occupied by a fractal particle $V_{occ} \sim R_p^3$, one finds $V_{occ} \sim R_g^3 \sim N^{3/D_f}$. The number of fractal particles in the system at any time, N_c, is related to the average mass of a particle by the conservation of mass: $N_c N = N_m$, where N_m is the constant number of monomers in the system. Thus the total volume of the system occupied by particles is $V_{occ,tot} = N_c V_{occ} \sim N^{3/D_f - 1}$. Since $D_f < 3$, the occupied volume fraction $f_{occ} = V_{occ,tot}/V_{system}$ increases without bound as the average particle size N increases. As f_{occ} approaches 1, the clusters begin to crowd each other and the system has evolved from a cluster-dilute to a cluster-dense state.

Even before the system becomes cluster-dense, the nearest-neighbor particle-particle distance R_{nn} quickly becomes a relevant length scale with respect to any given particle's motion, since it is this distance over which a particle must diffuse to collide and aggregate with another particle. At some intermediate time t where $0 < t < t(f_{occ,tot} = 1)$, one can estimate the characteristic diffusion velocity v as $v \sim D/R_{nn}$ with $R_{nn} \sim N_c^{-1/d}$ in d dimensions and N_c is the number of clusters in the system. As describe above, the product NN_c is equal to the total number of monomers in the system, hence it is a constant, thus one can equivalently write $R_{nn} \sim N^{1/d}$. One then finds that in the intermediate regime of the continuum limit, $K \sim N^{1/D_f - 1/d}$, which yields

$$\lambda = \frac{1}{D_f} - \frac{1}{d} \text{ (intermediate regime;Stokes-Einstein)}. \tag{18}$$

In the Epstein regime, similar arguments yield

$$\lambda = \frac{2}{D_f} - \frac{1}{d} - 2x \text{ (intermediate regime;Epstein)}. \tag{19}$$

In the continuum limit, with $D_f = 1.8$ and $d = 3$, Eq. (18) gives $\lambda = 0.22$, hence by Eq. (4) $z = 1.28$ in the intermediate regime. This value of the kinetic exponent z agrees well with recent simulation results [19]. As we show below, older simulation results [31] are also more consistent with the intermediate regime scaling than the dilute-limit scaling for various choices of the aggregation kernel. In a series of Monte Carlo simulations in two and three dimensions, Meakin *et al.* [31] modeled cluster-cluster aggregation with particle diffusion constants $D \sim N^\gamma$, where γ is related to the kernel homogeneity λ as

$$\lambda = \gamma + \frac{1}{D_f}. \tag{20}$$

For each γ used in their simulations, they fit their kinetic data (average cluster mass versus time) to a power-law growth curve to find the associated kinetic exponent, which we denote as z_{MC}. From the known value of γ (hence λ), we compute the kinetic exponent z from our scaling arguments—z_{dil} in the dilute limit and z_{int} in the intermediate regime. Our results listed in Table I clearly indicate that MC simulations for typical simulation monomer volume fractions ($f_v < 0.001$) do probe the intermediate scaling regime instead of the true dilute regime [32]. Thus, one needs to analyze simulations data for kinetic exponents in the Epstein regime both in terms of dilute and intermediate scaling exponents.

In Table II we summarize the predictions for λ in the various regimes.

TABLE I. In the first column, γ is the exponent for the mass dependence of the diffusion constant, $D \sim N^\gamma$. z_{MC} refers to the kinetic exponent as measured from a Monte Carlo simulation [33] using the indicated γ. z_{dil} and z_{int} are the dilute-limit and intermediate volume fraction theoretical predictions for the kinetic exponent using the corresponding γ.

γ	z_{MC}	z_{dil}	z_{int}
−3	0.33	0.29	0.31
−2	0.45	0.41	0.45
−1	0.8	0.69	0.82
−0.5	1.3–1.4	1.06	1.38

TABLE II. Predictions from our scaling theory as well as simulation results for the kinetic exponent in the various motional or concentration regimes. Here calculated values of λ are found from the corresponding scaling formula using $d=3$ (three-dimensional aggregation) and the values for D_f and x determined in the simulations for each regime. The fractal dimension of the aggregates, D_f is 1.8 for continuum and Epstein regimes and 1.9 for BLCA. The value of the mobility radius exponent, x, as defined in Eqs. (11) and (12), was found to be 0.46 for the Epstein regime simulations. The calculated value for the kinetic exponent z is found from λ (calculated) using Eq. (4). We find good agreement for each of these regimes. A single value for z (simulation) is given for the Epstein regime (both dilute and intermediate) since our simulations only explored a monomer volume fraction of 0.001, as stated in the paper.

Regime	λ (formula)	λ (calculated)	z (calculated)	z (simulation)
Ballistic	$(4-D_f)/2D_f$	0.55	2.2	~2.0
Continuum, dil.	0	0	1	1.0
Continuum, inter.	$(d-D_f)/dD_f$	0.22	1.28	1.25±0.25
Epstein, dil.	$(1-2xD_f)/D_f$	−0.36	0.73	0.80±0.02
Epstein, inter.	$(2d-D_f-2xdD_f)/dD_f$	−0.14	0.88	0.80±0.02

V. SIMULATION MODELS AND METHODS

In order to evaluate our theoretical predictions, we have run a series of Monte Carlo simulations for the Epstein regime. We start our simulation with 10^5 monomers placed in a cubical box (with periodic boundary conditions) of sufficient size to make the monomer volume fraction $f_v=0.001$. At each Monte Carlo step, one cluster is chosen at random with equal chances among all clusters and moved a maximum distance of one monomer diameter with a probability $p_{\text{move}}=D_{\text{clust}}/D_{\text{mon}}$ along a direction chosen randomly from a spherically uniform distribution. D_{clust} and D_{mon} are the Epstein diffusion constants of the cluster and monomer, respectively, as given by Eq. (8). The chosen cluster stays fixed with complimentary probability $1-p_{\text{move}}$. In the Epstein regime, $p_{\text{move}}=\pi a^2/A_{\text{CS}}$, where a is the radius of a monomer and A_{CS} is the cross-sectional area of the cluster. This ensures that monomers move with probability unity. A_{CS} is determined by a separate subroutine within the program that calculates the projected area of the cluster in a plane normal to the direction of motion. If a collision happens during a cluster movement, the colliding clusters are merged at the point of contact. Clusters are moved one at a time, and the Monte Carlo time in each case is incremented by N_c^{-1} for each attempted move, where N_c is the current number of clusters in the system. This sets a calibration for the simulation where one unit of Monte Carlo time corresponds to the time it takes for each primary particle to move on average one diameter in distance [19,30,31]. Our simulation results are averaged over a series of 10 runs.

The above method is the standard well-known prescription of Monte Carlo simulation of cluster-cluster aggregation. Using a variety of different kernels and within different motional regimes, the motion of both primary particles and fractal clusters is found to follow the correct diffusion law to a high degree of precision in all cases [2,19,31].

For purposes of comparison, we simulated aggregation under continuum DLCA and ballistic-limited cluster-cluster aggregation (BLCA) conditions in addition to Epstein DLCA. The continuum DLCA simulations are done identically to the Epstein ones with the replacement of the movement probability by $D_{\text{cluster}}/D_{\text{mon}}=R_{g0}/R_g$, where R_{g0} is the radius of gyration of a monomer and R_g is the chosen cluster's radius of gyration. For the BLCA simulations, the movement probability is 1, and the distance moved by a cluster during one time step (in units of the monomer diameter) is given by $N^{-1/2}$ according to the equipartition of energy. Upon formation, BLCA clusters are moved in a direction chosen randomly from a spherically uniform distribution. The cluster maintains this direction (straight line motion) for each subsequent movement until colliding and aggregating with another cluster, at which time the newly formed cluster again obtains a random direction of motion.

VI. CLUSTER PROJECTION AND MOBILITY RADII EXPONENTS

The predictions given above for λ require knowledge of the exponent x relating the mobility radius to the cluster mass. For this purpose, we display in Fig. 1 the log-log plots of A_{CS} versus N for Epstein clusters as well as for continuum DLCA and BLCA. Linear chains are also included as a test of the procedure. A database of 10 clusters of size N for $N=10,20,40,\ldots,640$ are generated for each kernel. For each cluster, 10^4 different, spherically random directions are chosen, and the cluster's projectional area normal to each direction is calculated. A grid scheme is used for this purpose with 15 grids per monomer diameter. The number 15 is chosen due to the fact that "gridding" a circle with grids 1/15 of a monomer diameter gives an area estimation that differs from the actual value by less than 0.1%. The $A_{\text{CS}}(N)$ for each kernel is an average over all the clusters of size N as well as each of the 10^4 directions for each cluster.

The linear chains exhibit $A_{\text{CS}}\sim N^{1.0}$, hence $x=0.5$. The exponent 1.0 does not indicate that no monomer-monomer screening occurs for linear chains; some degree of screening occurs for every projectional plane except those parallel to the line of the chain itself. What the value indicates is that the *average projectional cross-sectional area* as well as the amount of screening scale linearly with the size giving $x=0.50$, as expected.

For fractal clusters produced by each of the aggregation kernels, we find that $A_{\text{CS}}\sim N^{0.92}$, i.e., $x=0.46$. Meakin *et al.* [33] in a series of simulations have found such a simple power-law relationship between the cluster cross-sectional

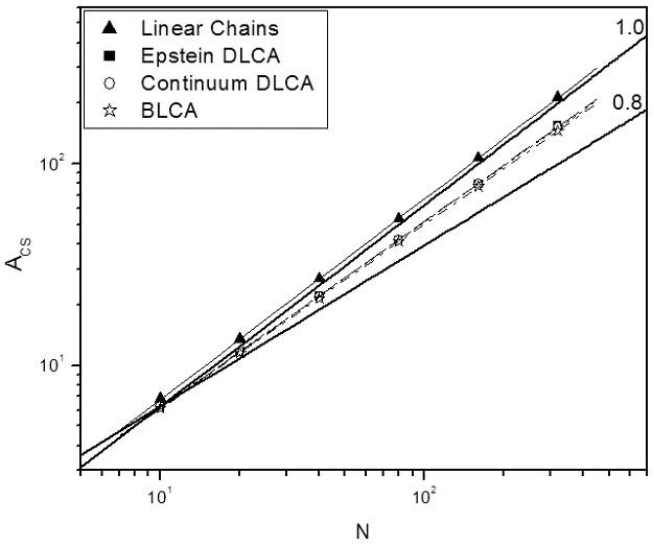

FIG. 1. Plot of the cluster projection A_{CS} vs. cluster particle number N. For Epstein and BLCA, $A_{CS}=\pi R_m^2$, where R_m is the cluster mobility radius. Linear chains have a power-law exponent of 0.995 ± 0.001, very close to the expected value of 1.000. All aggregates have exponents of ~ 0.92 (Epstein DLCA 0.928 ± 0.005, continuum DLCA 0.921 ± 0.003, BLCA 0.916 ± 0.002).

area and the particle number with an exponent of $2x\sim0.93$, very close to our finding of $2x=0.92$. These results are also in agreement with the finding of Wang and Sorensen for aggregates grown in the laboratory at high Kn [15]. Recently, Mackowski found the hydrodynamic radius of clusters with $D_f=1.7-2.0$ to scale with $x\sim0.47$, also consistent with our results [34].

VII. SIMULATION RESULTS IN THE EPSTEIN REGIME

A. Fractal dimension

In Fig. 2, we plot N versus R_g (in units of monomer diameter) for the Epstein clusters that were used in the projection calculations (10 each of mass 10,20,40,…,640). From the slope and intercept of this log-log plot, we find $D_f=1.80\pm0.06$ and $k_0=1.24\pm0.15$.

An alternate method for finding D_f makes use of the reciprocal space calculation of the geometric structure factor of large clusters. The structure factor is given by $S(\boldsymbol{q})=N^{-2}|\Sigma_i \exp(i\mathbf{q}\cdot\mathbf{r}_i)|^2$ where $\boldsymbol{q}$ is the scattered wave vector and $\boldsymbol{r}_i$ are the positions of the monomers within the cluster. A legitimate range of magnitudes for $\boldsymbol{q}$ is set by the length scales of the simulation, namely the monomer diameter d_0 and the linear size of the system box L such that $2\pi/L<q<2\pi/d_0$. $S(q)$ is an isotropic average of $S(\boldsymbol{q})$ over a large number of $\boldsymbol{q}$ vectors of magnitude q and spherically uniform random directions. At large wave vector q, the structure factor $S(q)$ of aggregates goes as q^{-D_f}, so D_f can be seen as the negative slope of a log-log plot of the structure factor of large clusters in the system at high q values [35]. Figure 3 shows the structure factor of the largest cluster in the system for the Epstein kernel at a time during the aggregation process where $N_c=97$. As can be seen, the structure factor curve

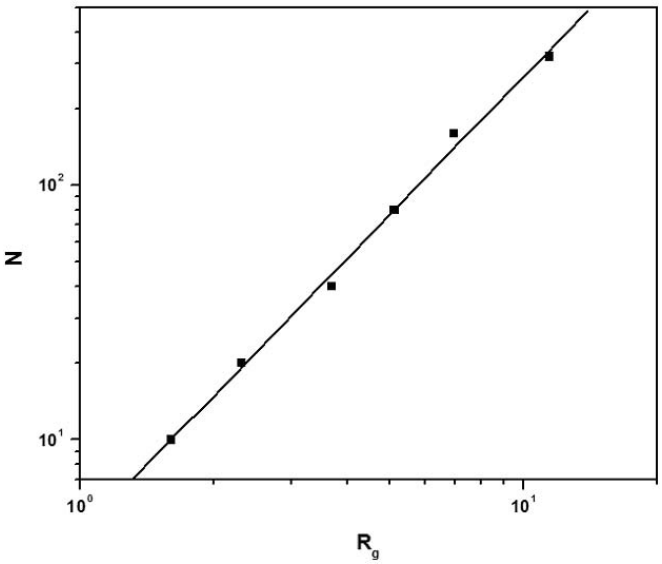

FIG. 2. The mass fractal dimension $D_f=1.80\pm0.06$ for Epstein aggregates as found from the real-space analysis of the ensemble of clusters. $k_0=1.24\pm0.15$.

for intermediate q values is well described by the fit line representing $S(q)\sim q^{-D_f}$ with $D_f=1.82\pm0.03$.

In Figs. 4(a)–4(d), we display images of the simulation box at various times in the simulation, showing the time evolution of the cluster morphologies for Epstein aggregates. Due to the similarity of the morphologies of clusters in all aggregation regimes (BLCA, continuum DLCA, Epstein DLCA) including D_f values that extend over the narrow range 1.8 to 1.9, morphologies alone cannot easily be used to distinguish the regime of aggregation.

B. Kinetics of aggregation

Figure 5 displays the results for the kinetics from our Epstein simulations. Here the scaled inverse cluster number

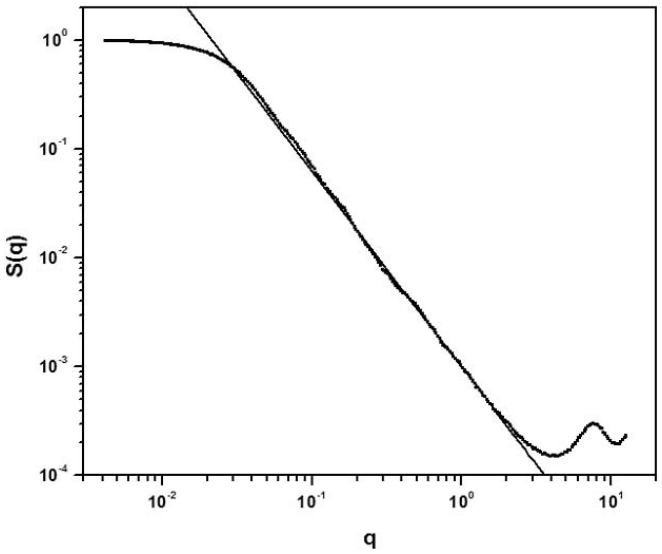

FIG. 3. The mass fractal dimension $D_f=1.82\pm0.03$ for Epstein aggregates as found from a structure factor calculation for large aggregates in the system.

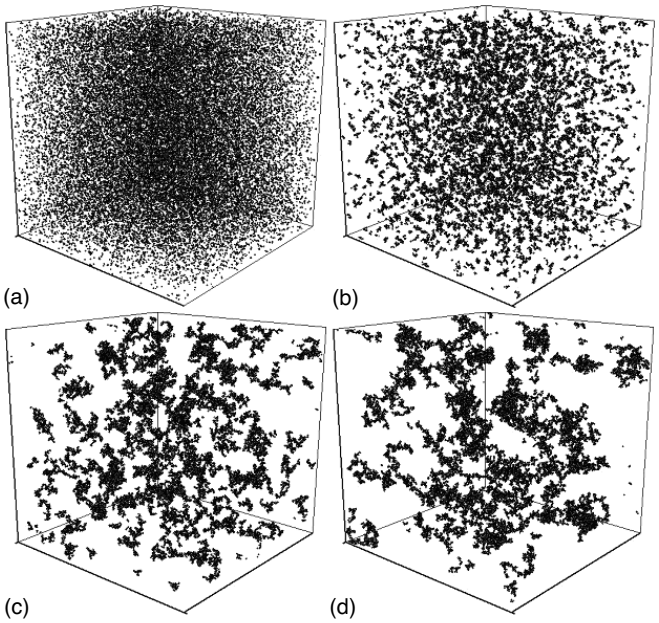

FIG. 4. (a) (top left)–(d) (bottom right) Images of the system volume at various times during aggregation in the Epstein regime. The average size of clusters and time are for (a) (N=260, t=2), (b) (N=32, t=9372), (c) (N=512, t=336 751), and (d) (N=2703, t =2 079 152).

is plotted versus Monte Carlo time in a log-log plot. The slope of this curve (after an initial transient) [36] corresponds to the kinetic exponent z, a value of $z=0.80\pm0.02$. Using the value of D_f determined above (1.8), scaling predictions [see Eqs. (17) and (19)] yield $z=0.73$ for the dilute limit and $z=0.88$ for the intermediate regime. The kinetic exponent from the simulation is consistent with these two values. As predicted by our scaling arguments above, our simulation results verify that the kinetic exponent for the Epstein regime

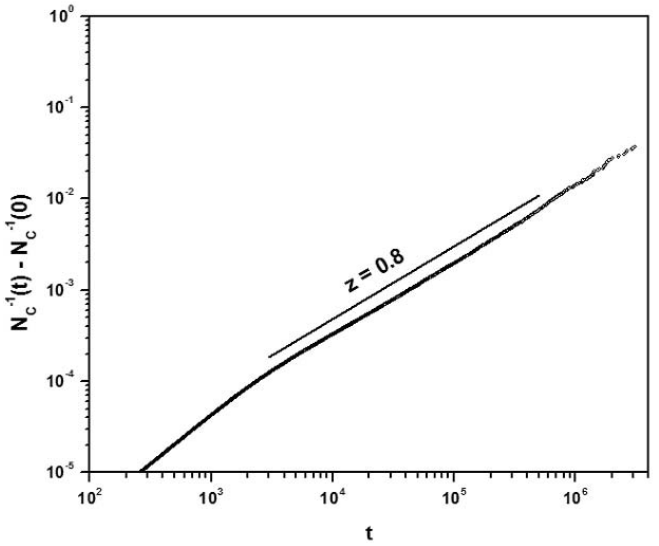

FIG. 5. The kinetic exponent starts with a transient value of z =1.0 [29] crossing over to a scaling regime value of $z=0.80\pm0.02$, a value well supported by theoretical calculations.

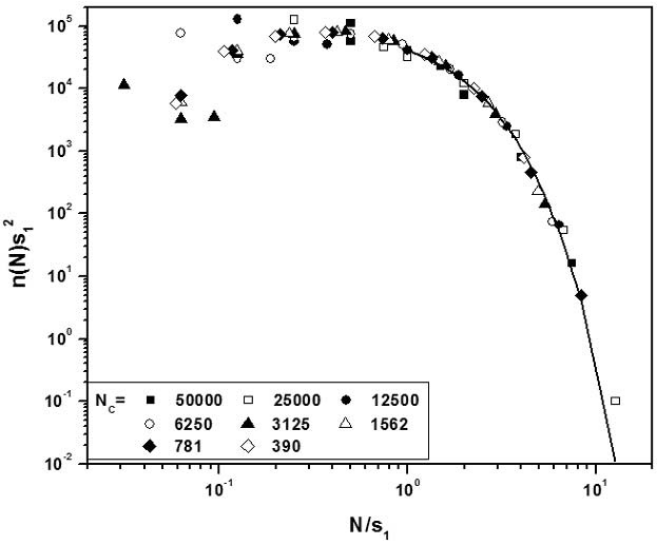

FIG. 6. Cluster size distribution data for a number of different times in the aggregation process. The system starts with 100 000 monomers and distributions are shown every time the number of clusters is halved, down to 390 clusters left in the system. The data for large $x=N/s_1$ (s_1 is the average cluster size) are well described by the scaling form $Ax^{-\lambda}e^{-\alpha x}$, where $\alpha=1-\lambda$ with $\lambda=-0.36\pm0.20$. The kinetics data yield $\lambda=-0.25\pm0.03$, in agreement with the size distribution data.

is both noticeably smaller than the continuum prediction of $z=1$ and well below the free molecular value of $z=2.2$.

In Table II, we display our calculated predictions for λ and z from our scaling theory along with simulation results for the kinetic exponent for the various motional or concentration regimes.

C. Cluster size distributions

As aggregation proceeds in a system, the cluster size distribution, which starts as monodisperse, develops a scaling form [15] that is written for large clusters as

$$n(N,t) = M_1 s_p^{-2} \varphi(x), \tag{21}$$

where $n(N,t)$ is the number of clusters of size N at time t, $M_i(t)$ is the ith moment of the distribution, $s_p=M_p/M_{p-1}$ is the pth average size, and $x=N/s_p$ is the scaling variable. The average size is independent of p for monodisperse systems. The scaled distribution has this functional form $\varphi(x)$ $=Ax^{-\lambda}e^{-\alpha x}$ with $\alpha=p-\lambda$ and $A=\alpha^{2-\lambda}/\Gamma(2-\lambda)$ for large x.

In Fig. 6, we have plotted the scaled size distributions for the Epstein regime for a number of simulation times. When the fit is made for the range $x>1$ (large x), excellent agreement with the scaling form is found for all times, as shown in Fig. 6. From the kinetics data above we found z $=0.80\pm0.02$ corresponding to a λ value of -0.25 ± 0.03. Fitting of the cluster size distributions to the scaled form [Eq. (21)] yields $\lambda=-0.36\pm0.20$, consistent with the kinetic results.

VIII. CONCLUSIONS

Monte Carlo simulations of dilute-limit aggregation of fractal aggregates in the Epstein regime have been carried out. We have found the mobility radius of Epstein aggregates calculated from particle projectional areas to scale with the particle mass with an exponent of 0.464 ± 0.003, in good agreement with both the computer simulations and experimental work of others.

Fractal dimensions for simulated Epstein aggregates were found to be 1.82 ± 0.03, close to that of continuum DLCA (~ 1.8) and BLCA (~ 1.9).

The kinetics exponent of aggregation in the Epstein regime from our simulations ($z=0.80$) is consistent with our scaling arguments ($z=0.73-0.88$). The cluster size distributions also agree well with both the kinetics and scaling results for large cluster sizes.

ACKNOWLEDGMENTS

Financial support given by NASA under Grant No. NNC04GA74G is gratefully acknowledged.

[1] S. K. Friedlander, *Smoke, Dust, and Haze: Fundamentals of Aerosol Behavior* (Wiley, New York, 1977).
[2] F. Family and D. P. Landau, *Kinetics of Aggregation and Gelation* (North-Holland, Amsterdam, 1984).
[3] T. T. Mercer, in *Fundamentals of Aerosol Science*, edited by D. T. Shaw (Wiley, New York, 1976), p. 85.
[4] P. E. Wagner and M. Kerker, J. Chem. Phys. **66**, 638 (1977).
[5] P. Meakin, J. Colloid Interface Sci. **102**, 505 (1984).
[6] P. Meakin, Adv. Colloid Interface Sci. **28**, 249 (1988).
[7] G. W. Mulholland, R. J. Samson, R. D. Mountain, and M. H. Ernst, Energy Fuels **2**, 481 (1988).
[8] W. W. Szymanski, A. Majerowicz, and P. E. Wagner, Aerosol Sci. Technol. **11**, 1 (1989).
[9] M. Y. Lin, H. M. Lindsay, D. A. Weitz, R. C. Ball, R. Klien, and P. Meakin, Nature (London) **339**, 360 (1989).
[10] M. Y. Lin, H. M. Lindsay, D. A. Weitz, R. C. Ball, R. Klein, and P. Meakin, Phys. Rev. A **41**, 2005 (1990).
[11] J. E. Martin, J. P. Wilcoxon, D. Schaefer, and J. Odinek, Phys. Rev. A **41**, 4379 (1990).
[12] T. Matsoukas and S. K. Friedlander, J. Colloid Interface Sci. **146**, 495 (1991).
[13] B. J. Olivier, C. M. Sorensen, and T. W. Taylor, Phys. Rev. A **45**, 5614 (1992).
[14] S. N. Rogak and R. C. Flagan, J. Colloid Interface Sci. **151**, 203 (1992).
[15] C. Oh and C. M. Sorensen, J. Aerosol Sci. **28**, 937 (1997).
[16] G. M. Wang and C. M. Sorensen, Aerosol Sci. Technol. **34**, 297 (2001).
[17] J. Cai, N. Lu, and C. M. Sorensen, J. Colloid Interface Sci. **171**, 470 (1995).
[18] C. M. Sorensen and G. C. Roberts, J. Colloid Interface Sci. **186**, 447 (1997).
[19] D. Fry, T. Sintes, A. Chakrabarti, and C. M. Sorensen, Phys. Rev. Lett. **89**, 148301 (2002).
[20] C. M. Sorensen, W. B. Hageman, T. J. Rush, H. Huang, and C. Oh, Phys. Rev. Lett. **80**, 1782 (1998).
[21] C. M. Sorensen, W. Kim, D. Fry, and A. Chakrabarti, Langmuir **19**, 7560 (2003).
[22] W. Kim, C. M. Sorensen, and A. Chakrabarti, Langmuir **20**, 3969 (2004).
[23] W. G. Kim, C. M. Sorensen, D. Fry, and Amit Chakrabarti, J. Aerosol Sci. **37**, 386 (2006).
[24] B. Dahneke, in *Theory of Dispersed Multiphase Flow*, edited by R. E. Meyer (Academic Press, New York, 1983).
[25] G. M. Hidy, *Aerosols: An Industrial and Environmental Science* (Academic Press, Orlando, FL, 1984).
[26] N. A. Fuchs, *The Mechanics of Aerosols* (Pergamon, Oxford, 1964).
[27] C. M. Sorensen and G. M. Wang, Aerosol Sci. Technol. **33**, 353 (2000).
[28] G. M. Wang and C. M. Sorensen, Phys. Rev. E **60**, 3036 (1999).
[29] M. Zurito-Gotor and D. E. Rosner, J. Colloid Interface Sci. **255**, 10 (2002).
[30] D. Fry, Ph. D. thesis, Kansas State University (2003).
[31] P. Meakin, T. Vicsek, and F. Family, Phys. Rev. B **31**, 564 (1985).
[32] Both dilute and intermediate scaling assumptions break down when $\gamma > 0$ as the system enters the cluster dense regime too quickly.
[33] P. Meakin, B. Donn, and G. W. Mulholland, Langmuir **5**, 510 (1989).
[34] D. W. Mackowski, J. Aerosol Sci. **37**, 242 (2006).
[35] C. M. Sorensen, Aerosol Sci. Technol. **35**, 648 (2001).
[36] All aggregation kernels are expected to have an initial transient period of linear growth, yielding $z=1$. This occurs because any system that starts as a monodisperse set of particles has very little change in the particle number or size distribution of clusters for the first few aggregation events. For example, the system during the tenth aggregation event looks almost identical to the system during the first aggregation, thus the rate must be approximately the same (linear growth rate). Only when the initial size distribution and number of clusters has significantly changed can the exponent switch over to a different steady-state value.